REVISION 2

Word Count: 3363 (with references and captions to figures)

Word Count: 2476 (text only with an abstract)

First find of merrillite $Ca_3(PO_4)_2$ in a terrestrial environment as an inclusion in lower-mantle diamond

Felix V. Kaminsky[1,1], Dmitry A. Zedgenizov[2]

[1]Vernadsky Institute of Geochemistry and Analytical Chemistry, Russian Academy of Sciences, Kosygin Street 19, Moscow 119334, Russian Federation

[2] Zavaritsky Institute of Geology and Geochemistry, Ural Branch of the Russian Academy of Sciences, Ekaterinburg, 620016, Russia

ABSTRACT

Merrillite, ideally $Ca_{18}Na_2Mg_2(PO_4)_{14}$ (Dana No: 38.03.04.04 Strunz No: 08.AC.45), an analogue to synthetic tricalcium phosphate β-$Ca_3(PO_4)_2$, was identified as an inclusion in lower-mantle diamonds from the Rio Soriso area, Brazil. It was associated with former bridgmanite, CaSi- and CaTi-perovskites, and ferropericlase. This is the first report of merrillite in a terrestrial environment; previously, it was known only in meteorites and Lunar rocks. The compositions of merrillite vary in different localities; the Rio Soriso sample was enriched in SO_3 (2.03 wt.%). Merrillite from lower-mantle diamonds may be a retrograde phase of the tuite (γ-$Ca_3(PO_4)_2$).

[1] Corresponding author. E-mail: felixvkaminsky@aol.com. ORCID: 0000-0001-6035-7114.

Owing to their crystal structures, both merrillite and tuite may be important potential hosts for rare earth elements (REE) and large ion lithophile elements (LILE), including Sr and Ba, in the deep Earth. The find of merrillite suggests a larger variety of mineral species in the lower mantle than previously assumed.

Keywords: merrillite, tuite, whitlockite, diamond, phosphates, lower mantle, Raman spectra

Introduction

Phosphorus is a minor element on Earth, particularly in its deep interior. The average concentration of phosphorus in the Earth's mantle is 90 ppm, or 0.021 P_2O_5, which is almost eight times less than that in the bulk Earth (McDonough and Sun, 1995; McDonough, 2014). It has been suggested that most terrestrial phosphorus resides in the lower mantle (Nash, 1994). Under normal oxidative conditions, phosphorus crystallizes as phosphate. However, phosphates are rare minerals in the mantle.

Previously, we reported apatite and two unnamed orthorhombic phosphates, mixed-anion phosphate $Na_4Mg_3(PO_4)_2(P_2O_7)$ and Fe-diphosphate $Fe_2Fe_5(P_2O_7)_4$ as members of the Earth's lower-mantle natrocarbonatitic association and found as inclusions in diamonds from the Juina area, Brazil (Kaminsky et al., 2013, 2016). This association represents the near-solidus melt, which has a carbonate-phosphate composition, stimulating the formation of diamond in the deep Earth (Ryabchikov and Hamilton, 1994).

During the study of possible lower-mantle diamonds from the Juina area (Mato Grosso State, Brazil) and their inclusions, we identified several grains of Ca-phosphate in association

with enstatite, breyite, and ferropericlase (Fe-rich periclase - Per68Wüs32). We suggest that enstatite and breyite are retrograde transformation products of bridgmanite and davemaoite. Detailed examination of these phosphate grains with the use of Raman spectroscopy indicated that they were merrillite, an analogue to synthetic tricalcium phosphate β-$Ca_3(PO_4)_2$ with an ideal formula $Ca_{18}Na_2Mg_2(PO_4)_{14}$ (Dana No: 38.03.04.04; Strunz No: 08.AC.45).

Merrillite (which we will describe below as β-$Ca_3(PO_4)_2$) is a major accessory phosphate in meteorites and Lunar rocks (Wherry, 1917; Fuchs, 1969; Hughes et al., 2006, 2008; Jolliff et al., 2006; https://www.mindat.org/min-6577.html) but virtually unknown in the Earth's rocks, although minor admixture of merrillite component has been found in terrestrial whitlockite (Hughes et al., 2008). An Fe-dominant analogue of merrillite, identified as a separate mineral species in several Martian meteorites (shergottites), was named ferromerrillite (Britvin et al., 2016).

Below, we present characteristics of the first terrestrial finding of merrillite in diamonds from the alluvial deposits of Juina area (Brazil).

Samples and Methods

Alluvial diamonds from Rio Soriso in the Juina area (Mato Grosso State, Brazil) were previously studied by Hayman et al. (2005). A set of oxide minerals (ferropericlase, CaSi-perovskite, bridgmanite, unknown phase of SiO_2, and others) was identified as inclusions in diamonds; their origin was suggested as being at depths of the Earth's lower mantle (Hayman et al., 2005). In addition to those earlier minerals found in the current study, we found more inclusions in the Rio Soriso diamonds, – not only oxides, but also magnesite and phosphate.

Phosphates were identified in two samples, #3.6.2, and #3.10.2. In sample #3.6.2, it occurred as a single elongated inclusion, approximately 40 μm in size (Fig. 1a). In sample #3.10.2, phosphate formed a chain of five tabular, elongated inclusions, 15-50 μm in size (Fig. 1b), in association with ferropericlase with $f = 0.32$.

Prior to analyses, samples were polished to expose the inclusions. Exposed individual inclusions were identified in electron backscattering mode (BSE) using a focused electron beam (15 kV, 10 nA) and an acquisition time of 30-60 s. Mineral inclusions were analyzed using an Oxford energy-dispersive X-ray spectrometer (EDS XMax 80) attached to a Tescan MIRA 3 LMU scanning electron microscope (at IGM SB RAS). Chemical compositions (without P_2O_5 and SO_3 concentrations) were also determined using a JEOL JXA-8100 EPMA, equipped with five wavelength dispersive spectrometers and an energy dispersive (EDX) spectrometer at an accelerating voltage of 20 kV, beam current of 20 nA, and beam diameter of 1 μm. The full protocol of the EMPA was described by Lavrent'ev et al. (2015).

Raman spectra were collected using a Horiba Jobin Yvon LabRAM HR800 Raman microspectrometer equipped with a 532-nm Nd:YAG laser and an Olympus BX41 microscope at ×50 magnification. Spectra were recorded at room temperature in a backscattering geometry in the range 100 to 1200 cm^{-1} with a spectral resolution of approximately 1 cm^{-1}. The spectra were calibrated using the 520.6 cm^{-1} line of a silicon wafer. The wavenumbers were accurate to ±1 cm^{-1}.

Carbon isotopic ratios were measured using a Flash EA 1112 (Thermo Fisher Scientific) coupled to a Finnigan Delta Plus XP isotope-ratio mass spectrometer. The diamonds were crushed in an agate mortar, and diamond fragments of approximately 50–100 μm were inserted into Sn capsules and dropped into the combustion reactor (1020 °C). The temperature of

the reduction reactor was maintained at 650 °C. All carbon isotopic compositions of the samples are reported in standard δ notation on the VPDB scale ($\delta^{13}C_{VPDB}$). Two to five fragments of each sample were analyzed to calculate the average and standard deviation (1σ).σ) values.

Results

Composition

The compositions of phosphate inclusions are presented in Table 1.

There were noticeable differences in the compositions of the phosphate samples from the two diamonds. The grain from sample #3.6.2 contained almost 3 % MgO, while this element was not identified in any grain from sample #3.10.2. Sample #3.6.2 was also twice as rich in Fe than sample #3.10.2. In contrast, concentrations of alkalis (Na, K) in sample #3.10.2 were more than one order of magnitude higher than those in sample #3.6.2. Low totals suggest the presence of other elements that were not analyzed in the mineral. Of particular interest was the high concentration of sulfur in all grains from sample #3.10.2, which was not observed in previous analyses of Ca-phosphates. In contrast to the phosphates from the Suizhou chondrite from the Hubei province in China (Xie et al., 2002), Rio Soriso samples were enriched in Fe.

Raman spectra

The Raman spectra of the phosphate inclusions, performed at IGM SO RAN, are presented in Figure 2. We observed a number of vibrations with modes at 407, 960, 973, and 1080 cm^{-1} from sample #3.6.2, and 217, 404, 443, 473, 607, 965, 970, and 1065 cm^{-1} from sample #3.10.2. These mode energies correspond almost exactly the Raman shifts of merrillite from the Suizhou

meteorite (Xie et al., 2002) whereas they differ significantly from the Raman spectrum of tuite (Xie et al., 2002; Zhai et al., 2010). The most prominent peak at 956 cm^{-1} (960 cm^{-1} in sample 3.6.2) with a shoulder at 970 cm^{-1} (973 in sample 3.6.2) is assigned to the ν1 symmetric stretching vibration of the PO_4 group, while the peaks at 1065 and 1080 cm^{-1} is assigned to the ν3 asymmetric stretching vibration of PO_4. The small peak at 607 cm^{-1} from some grains can be assigned to the ν4 bending mode, and peaks at less than 480 cm^{-1} with the lattice modes. Based on the Raman spectroscopic measurements, we conclude that the phosphate phase from the lower-mantle diamond found in the Soriso area, Brazil show the same arrangement of phosphate groups as the β-$Ca_3(PO_4)_2$ phase, that is, the phosphate from Rio Soriso diamonds can be attributed to merrillite. The peak at ~923 cm^{-1} that is present in terrestrial whitlockite and is attributed to the P-O stretch for the hydroxyl oxygen in the hydrogen phosphate group (e.g., McCubbin et al., 2018) is missing from the spectra of studied samples and is the strongest evidence that this is merrillite and not whitlockite.

Carbon isotopic composition

The carbon isotopic compositions $\delta^{13}C$ in diamonds enclosing merrillite are 5.56 ± 0.54 ‰ VPDB (sample #3.6.2) and 5.59 ± 0.45 (sample #3.10.2), very close to the average values for the lower mantle values of $\delta^{13}C$ (Kaminsky, 2017), and within suggested average mantle range of $\delta^{13}C$ values (Galimov, 1984).

Discussion

There are four polymorphs known to-date in the $Ca_3(PO_4)_2$ system, denoted as α′-, α-, β-, and γ-phases. The β-phase (merrillite) is stable under ambient conditions, the γ-phase (tuite) is stable at high pressures, and the α′- and α-phases are stable at high temperatures (Sugiyama and Tokonami, 1987; Xie et al. 2003).

The Rio Soriso merrillite grains are the first finding of this mineral in a terrestrial environment. The hosting diamonds from this location contain, in addition to merrillite, mineral inclusions of $MgSiO_3$ (possibly, orthopyroxene which we believe to be the result of back-transformation of bridgmanite), $CaSiO_3$ (possibly, breyite which we believe to be the result of back-transformation of davemaoite, former CaSi-perovskite), $Ca(Si,Ti)O_3$ phase, ferropericlase, and magnesite, minerals from peridotitic and carbonatitic lower-mantle associations (Kaminsky, 2017). On this basis, Rio Soriso diamonds have been proposed to have formed in the lower mantle (e.g., Hayman et al., 2005), and accordingly present inclusions of merrillite may have been initially the high-pressure mineral tuite γ-$Ca_3(PO_4)_2$, which is stable to at least up to 35.4 GPa under 1300 K (Zhai et al. 2013), i.e., may have crystallized at the lower-mantle conditions. In Rio Soriso diamond #3.10.2, $Ca_3(PO_4)_2$ was associated with high-Ni ferropericlase, that is, its formation may be attributed to the upper part of the lower mantle with pressures above 24 GPa (Kaminsky and Lin, 2017).

It may be suggested that the merrillite, as diamond inclusion, may be a retrograde transformation product of the high-pressure γ-$Ca_3(PO_4)_2$ phase, tuite, stable within pressure limits of 12-35 GPa (Sugiyama and Tokanami, 1987; Zhai et al., 2013). It may be proposed that tuite was initially formed in the lower-mantle natrocarbonatitic media, which, in addition to carbonates, halides, fluorides, and other minerals, contains also phosphates, such as apatite, and two new, still-unnamed minerals $Na_4Mg_3(PO_4)_2(P_2O_7)$ and $Fe_2Fe_5(P_2O_7)_4$ (Kaminsky et al., 2013,

2016), and transformed into merrillite during the ascent of hosting diamonds to the surface. Experiments demonstrate the merrillite – tuite transformation at 4 GPa and 950 °C (Roux et al., 1978), or even at 23 GPa (Xie et al., 2002, 2003), i.e., within the transition zone or the upper mantle conditions.

Structurally, both tuite and merrillite belong to a vast group of compounds with a palmierite-type structure and the general chemical formula $M_3(XO_4)_2$, where M = Ba, Sr, Ca, Pb, Rb, K, Na, NH_4, Tl, REE, and X = V, Cr, P, S, and As. The X cation in the palmierite-type structure is tetrahedrally coordinated, whereas the M cations occupy two symmetrically non-equivalent sites, M1 and M2. The M1 site displays a (6+6) coordination, with six M1-O bond lengths markedly shorter than the other six M1-O bonds. In contrast, the M2 site is 10-coordinated (Thompson et al. 2013). Both tuite and merrillite are trigonal structure, belonging to *R*3–*m* space group. The structure of synthesized γ-$Ca_3(PO_4)_2$ was determined by Sugiyama and Tokonami (1987) using a sample made from hydroxylapatite at 12 GPa and 1100-2300 °C. They demonstrated that tuite has a 12-coordinated Ca(1) site and a 10-coordinated Ca(2) site. In the structure of $Ca_3(PO_4)_2$, a phosphorus atom is tetrahedrally coordinated by oxygen atoms, and calcium atoms occupy two types of large metal sites. The Ca(l) site has 12 oxygen neighbors, while the other Ca(2) site is coordinated by 10 oxygen atoms.

Merrillite has another compositional analogue, hydroxyl-containing whitlockite $Ca_9(MgFe)(PO_4)_6PO_3OH$, which has different of merrillite space group *R*3*c*. It has been known since the mid-20th century in granitic pegmatites, phosphate rock deposits, organic materials, and even in guano caves (Wurster et al., 2015). After the discovery of hydroxyl-free $Ca_3(PO_4)_2$ phosphate in meteorites, Dowty (1977) recommended the use the name of merrillite for the extraterrestrial variety on the basis that the lack of H led to a fundamental structural difference

between the extraterrestrial and terrestrial varieties, and merrillite was revalidated by the Commission on New Minerals, Nomenclature and Classification of the International Mineralogical Association (IMA) at that time (Jolliff et al., 2006). More recently McCubbin et al. (2014) studied merrillite in meteorites and found no hydrogen in those samples as well. They concluded that natural merrillite have no whitlockite component as a consequence of the limited thermal stability of H in whitlockite (stable only at T < 1050 ºC), which would prohibit merrillite-whitlockite solid-solution at high temperatures.

The major and trace element compositions of the inclusions of Ca minerals in superdeep diamonds indicate that they crystallized from Ca-carbonatite melts that were derived from partial melting of eclogite bodies in deeply subducted oceanic crust in the transition zone or even the lower mantle (Zedgenizov et al., 2016). The discovery of phosphate inclusions in association with superdeep minerals (ferropericlase and suggested bridgmanite, CaSi-perovskite, and stishovite) cannot only provide additional support for their role in the diamond formation, but also help to define additional mantle reservoirs involved in the global geodynamic cycle. Owing to their crystal structure, both tuite and merrillite in the lower mantle may be important potential hosts for rare earth elements (REE) and large ion lithophile elements (LILE), such as Sr and Ba (Murayama et al., 1986; Sugiyama and Tokonami, 1987; Xie et al., 2003; Zhai et al., 2010). Our analyses of merrillite show 1.61 wt.% SrO (Table 1), confirming this.

Implications

The finding of merrillite $Ca_3(PO_4)_2$ in the terrestrial environment in association with mineral phases that are potentially backtransformed lower-mantle minerals, indicates a complex

composition of the Earth's lower mantle. This finding suggests a larger variety of mineral species in the lower mantle than previously assumed, not limited only by rock-forming minerals, including bridgmanite, CaSi-perovskite, ferropericlase, stishovite, and some accessory phases (particularly of the natrocarbonatitic association) found previously (e.g., Kaminsky 2017 and references therein). Further studies on lower-mantle samples should provide additional interesting findings.

The behavior of phosphate minerals in the deep earth is of great interest for understanding the behavior of REEs and LILEs. Phosphates stable in the deep Earth could be important hosts of REE, Na, Sr, and Ba.

Acknowledgements

We thank Nastya Kalugina for her help with the Raman measurements, O. Tschauner and an anonymous reviewer for their very valuable, constructive criticism, which helped us to improve the manuscript.

Funding

Sample preparation, chemical analyses, and Raman measurements of inclusions were supported by the Russian Foundation for Basic Research (grant No. 21-55-50011).

References cited

Boesenberg, J.S., Delaney, J.S., and Hewins, R.H. (2012) A petrological and chemical re-examination of Main Group pallasite formation. *Geochimica et Cosmochimica Acta,* 89, 134-158.

Britvin, S.N., Krivovichev, S.V., and Armbruster, T. (2016) Ferromerrillite, $Ca_9NaFe^{2+}(PO_4)_7$, a new mineral from the Martian meteorites, and some insights into merrillite-tuite transformation in shergottites. European Journal of Mineralogy, 28, 125-136. DOI: 10.1127/ejm/2015/0027-2508.

Dowty, E. (1977) Phosphate in Angra dos Reis: Structure and composition of the $Ca_3(PO_4)_2$ minerals. Earth and Planetary Science Letters, 35, 347-351.

Fuchs, L.H. (1969) The phosphate mineralogy of meteorites. Astrophysics and Space Science Library, 12, 683–695.

Galimov, E.M. (1984). The relation between formation conditions and variations in isotope composition of diamond. Geochemistry International 22, 118-141.

Jolliff, B.L., Hughes, J.M., Freeman, J.J., Zeigler, R.A. (2006) Crystal chemistry of lunar merrillite and comparison to other meteoritic and planetary suites of whitlockite and merrillite. American Mineralogist, 91, 1583-1595. DOI: 10.2138/am.2006.2185.

Hayman, P.C., Kopylova, M.G., and Kaminsky, F.V. (2005) Lower mantle diamonds from Rio Soriso (Juina, Brazil). Contributions to Mineralogy and Petrology, 149, 430-445. DOI: 10.1007/s00410-005-0657-8.

Hughes, J.M., Jolliff, B.L., and Gunter, M.E. (2006) The atomic arrangement of merrillite from the Fra Mauro Formation, Apollo 14 lunar mission: The first structure of merrillite from the Moon. American Mineralogist, 91, 1547–1552.

Hughes, J.M., Jolliff, B.L., and Rakovan, J. (2008) The crystal chemistry of whitlockite and merrillite and the dehydrogenation of whitlockite to merrillite. American Mineralogist, 93, 1300–1305.

Jolliff, B.L., Hughes, J.M., Freeman, J.J., Zeigler, R.A. (2006) Crystal chemistry of lunar merrillite and comparison to other meteoritic and planetary suites of whitlockite and merrillite. American Mineralogist, 91, 1583–1595.

Kaminsky, F.V. (2017) The Earth's Lower Mantle: Composition and Structure. Springer, 331 pp. DOI: 10.1007/978-3-319-55684-0.

Kaminsky, F.V., Lin, J.-F. (2017) Iron partitioning in natural lower-mantle minerals: Toward a chemically heterogeneous lower mantle. American Mineralogist, 102, 824-832. DOI: 10.2138/am-2017-5949.

Kaminsky, F.V., Wirth, R., and Schreiber, A. (2013) Carbonatitic inclusions in Deep Mantle diamond from Juina, Brazil: new minerals in the carbonate-halide association. Canadian Mineralogist, 51, 669–688. DOI: 10.3749/canmin.51.5.669.

Kaminsky, F.V., Ryabchikov, I.D., and Wirth, R. (2016) A primary natrocarbonatitic association in the Deep Earth. Mineralogy and Petrology, 110, 387-398. DOI: 10.1007/s00710-015-0368-4.

Lavrent'ev, Y.G., Karmanov, N.S., and Usova, L.V. (2015) Electron probe microanalysis of minerals: Microanalyzer or scanning electron microscope? Russian Geology and Geophysics, 56, 1154–1161.

McCubbin, F.M., Shearer, C.K., Burger, P.V., Hauri, E.H., Wang, J.H., Elardo, S.M., and Papike, J.J. (2014) Volatile abundances of coexisting merrillite and apatite in the martian

meteorite Shergotty: Implications for merrillite in hydrous magmas. American Mineralogist, 99, 1347–1354. DOI: 10.2138/am.2014.4782.

McCubbin, F.M., Phillips, B.L., Adcock, C.T., Tait, K.T., Steele, A., Vaughn, J.S., Fries, M.D., Atudorei, V., Vander Kaaden, K.E., and Hausrath, E.M. (2018) Discreditation of bobdownsite and the establishment of criteria for the identification of minerals with essential monofluorophosphate (PO_3F^{2-}). American Mineralogist 103, 1319-1328. DOI: 10.2138/am-2018-6440.

McDonough, W.F. (2014) Compositional Model for the Earth's Core. In R.W. Carlso, Ed., Treatise on Geochemistry, 2nd ed., 3, p. 559–576. Elsevier.

McDonough, W.F., and Sun, S.-S. (1995) Composition of the Earth. Chemical Geology 120, 223–253, DOI:10.1016/0009-2541(94)00140-4.

Murayama, J.K., Nakai, S., Kato, M., and Kumazawa, M. (1986) A dense polymorph of $Ca_3(PO_4)_2$: a high pressure phase of apatite decomposition and its geochemical significance. Physics of the Earth and Planetary Interiors, 44, 293–303.

Nash W.P. (1984) Phosphate minerals in terrestrial igneous and metamorphic rocks. In: Nriagu J.O., Moore P.B. (eds) Phosphate Minerals, p. 215-241. Springer, Berlin, Heidelberg. DOI: 10.1007/978-3-642-61736-2_6.

Roux, P., Lowor, D., and Bonel, G. (1978) Sur une novella forme cristallite du phosphate tricalcique. Comptes Rendus de l'Académie des Sciences. Série C, 286, 549-551.

Ryabchikov, I.D., and Hamilton, D.L. (1994) Near-solidus melts in carbonatized mantle peridotites in the presence of apatite and uraninite. Geochemistry International, 31(3), 77-85.

Sugiyama, S., and Tokonami, M. (1987) Structure and crystal chemistry of a dense polymorph of tricalcium phosphate $Ca_3(PO_4)_2$: a host to accommodate large lithophile elements in the Earth's mantle. Physics and Chemistry of Minerals, 15, 125-130. DOI: 10.1007/BF00308774.

Thompson, R.M., Xie, X., Zhai, S., Downs, R.T., and Yang, H. (2013) A comparison of the $Ca_3(PO_4)_2$ and $CaSiO_3$ systems, with a new structure refinement of tuite synthesized at 15 GPa and 1300 ºC. American Mineralogist, 98, 1585-1592. DOI: 10.2138/am.2013.4435.

Wherry, E.T. (1917) Merrillite, meteoritic calcium phosphate. American Mineralogist, 2, 119.

Wurster, C.M., Munksgaard, N., Zwart, C., and Bird, M. (2015) The biogeochemistry of insectivorous cave guano: a case study from insular Southeast Asia. Biogeochemistry, 124, 163-175. DOI: 10.1007/s10533-015-0089-0.

Xie, X., Minitti, M.E., Chen, M., Mao, H.K., Wang, D., Shu, J., and Fei, Y. (2002) Natural high-pressure polymorph of merrillite in the shock vein of the Suizhou meteorite. Geochimica et Cosmochimica Acta, 66, 2439-2444.

Xie, X., Minitti, M.E., Chen, M., Mao, H.-K., Wang, D., Shu, J., and Fei, Y. (2003) Tuite, □-$Ca_3(PO_4)_2$: a new mineral from the Suizhou L6 chondrite. European Journal of Mineralogy, 15, 1001-1005. DOI: 10.1127/0935-1221/2003/0015-1001.

Zedgenizov, D.A., Ragozin, A.L., Kalinina, V.V., and Kagi, H. (2016) The mineralogy of Ca-rich inclusions in sublithospheric diamonds. Geochemistry International, 54 (10), 890-900.

Zhai, S., Wu, X., and Ito, E. (2010) High-pressure Raman spectra of tuite, γ -$Ca_3(PO_4)_2$. Journal of Raman Spectroscopy, 41, 1011-1013. DOI: 10.1002/jrs.2522.

Captions to figures:

Figure 1. Inclusions of phosphate $Ca_3(PO_4)_2$ in diamonds from the Rio Soriso area. (**a**) sample #3.6.2; (**b**) sample #3.10.2.

Figure 2. Raman spectra of merrillite. (**a**) from sample #3.6.2; (**b**) from sample #3.10.2.

This is the peer-reviewed, final accepted version for American Mineralogist, published by the Mineralogical Society of America.
The published version is subject to change. Cite as Authors (Year) Title. American Mineralogist, in press.
DOI: https://doi.org/10.2138/am-2022-8175. http://www.minsocam.org/

Table 1. Chemical compositions of merrillite.

Component	Inclusions in diamond						Suizhou chondrite		Tip Top pegmatite
	Sample #3.6.2	Sample #3.10.2 (in association with high-Ni ferropericlase)					Merrillite	Tuite	Whitlockite
	3.6.2c	3.10.2d1	3.10.2d2	3.10.2d3	3.10.2d4	Av. of 4		Av. of 3	
	This work						Xie et al., 2003		Hughes et al., 2008
Oxides									
SiO_2	0.05	0.01	0.02	0.00	0.06	0.02	n.a.	n.a.	<0.02
TiO_2	0.08	0.00	0.00	0.00	0.00	0.00	0.06	0.04	n.a.
Al_2O_3	0.10	0.02	0.00	0.03	0.01	0.02	n.a.	n.a.	<0.01
Cr_2O_3	0.00	0.03	0.01	0.03	0.00	0.02	0.03	0.00	n.a.
FeO	2.07	1.45	0.85	0.33	2.16	1.19	0.28	0.38	<0.06
NiO	0.01	0.00	0.00	0.01	0.01	0.01	0.08	0.05	n.a.
MnO	0.08	0.12	0.16	0.08	0.12	0.12	n.a.	n.a.	<0.06
MgO	2.95	0.00	0.00	0.00	0.00	0.00	3.27	3.58	3.61
CaO	48.4	48.7	47.6	49.0	40.3	46.4	46.6	46.14	46.6
SrO*	n.a.	n.a.	1.61	n.a.	n.a.	1.61	n.a.	n.a.	0.31
Na_2O	0.08	3.26	1.77	0.83	1.81	1.92	2.57	2.80	0.46
K_2O	0.04	1.16	0.73	0.22	0.43	0.63	0.03	0.07	n.a.
P_2O_5*	44.18	42.9	44.9	n.a.	n.a.	43.9	47.7	47.16	46.0
SO_3*	n.a.	2.43	1.62	n.a.	n.a.	2.03	n.a.	n.a.	0.07
F	n.a.	n.a.	n.a.	n.a.	n.a.	n.a.	n.a.	n.a.	0.43
H_2O	n.a.	n.a.	n.a.	n.a.	n.a.	n.a.	n.a.	n.a.	0.84
Total	98.04	100.08	99.27	50.53	44.90	97.87	100.61	100.22	98.2**
Atoms									
Fe	0.029	0.020	0.012	0.005	0.030	0.017	0,004	0.005	–
Mg	0.073	0	0	0	0	0	0.081	0.089	0.090
Ca	0.863	0.869	0.849	0.874	0.718	0.827	0.831	0.822	0.831
Sr	–	–	0.016	–	–	0.016	–	–	0.003
Na	0.003	0.103	0.057	0.027	0.058	0.063	0.083	0.090	0.014
K	0	0.024	0.016	0.004	0.010	0.014	0	0.002	–
P	0.622	0.594	0.632	–	–	0.618	0.672	0.664	0.647
S	–	0.030	0.040	–	–	0.025	–	–	0.001
Fe/(Fe+Mg)	0.284	–	–	–	–	–	–	0.053	–
Total	1.590	1.650	1.622	0.910	0.816	1.580	1.626	1.672	1.586

Note: * EDS analysis. n.a. – not analyzed;
** Incl. Y_2O_3 (<0.05) and Ce_2O_3 (<0.09).

Figure 1a

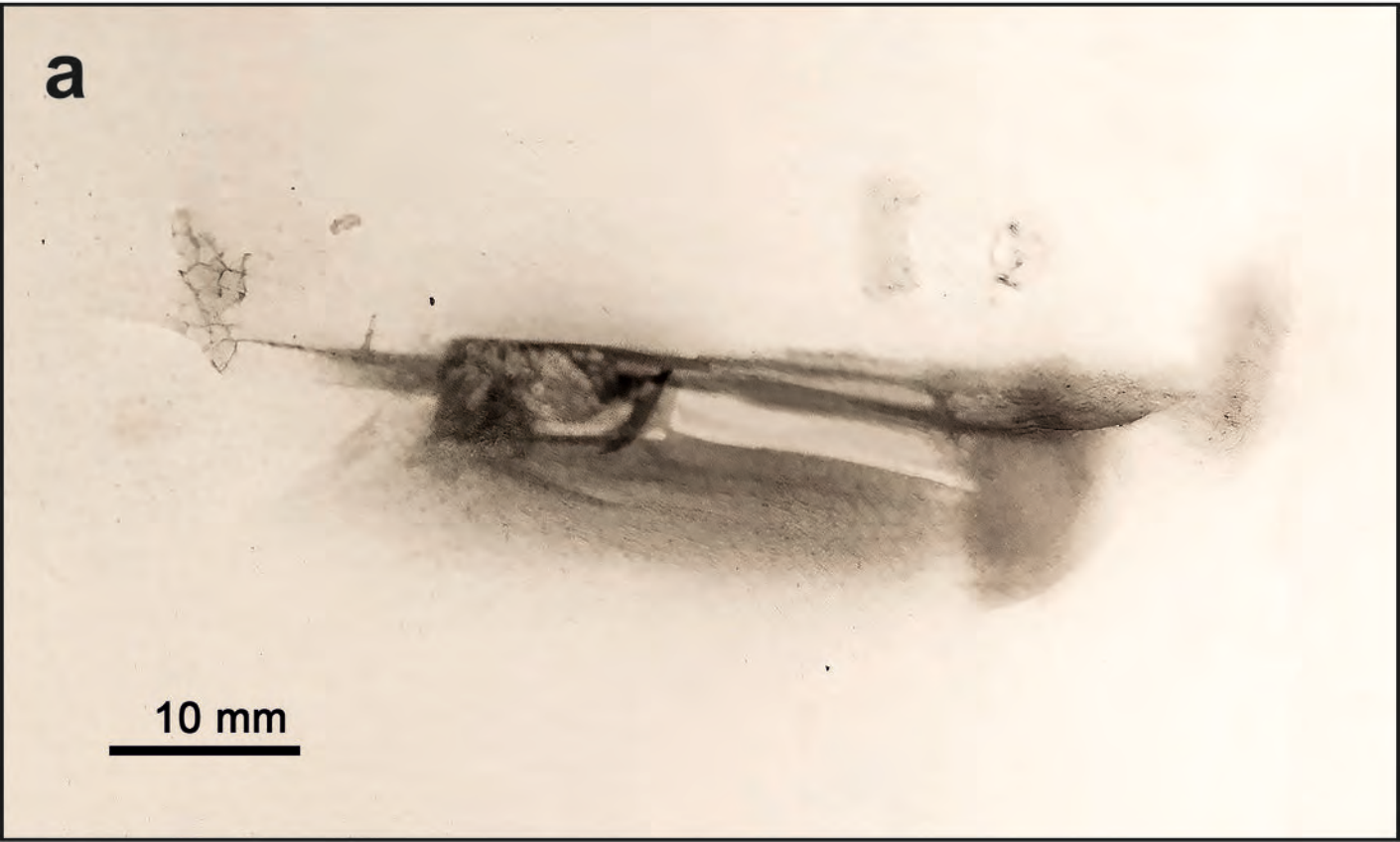

Figure 1b

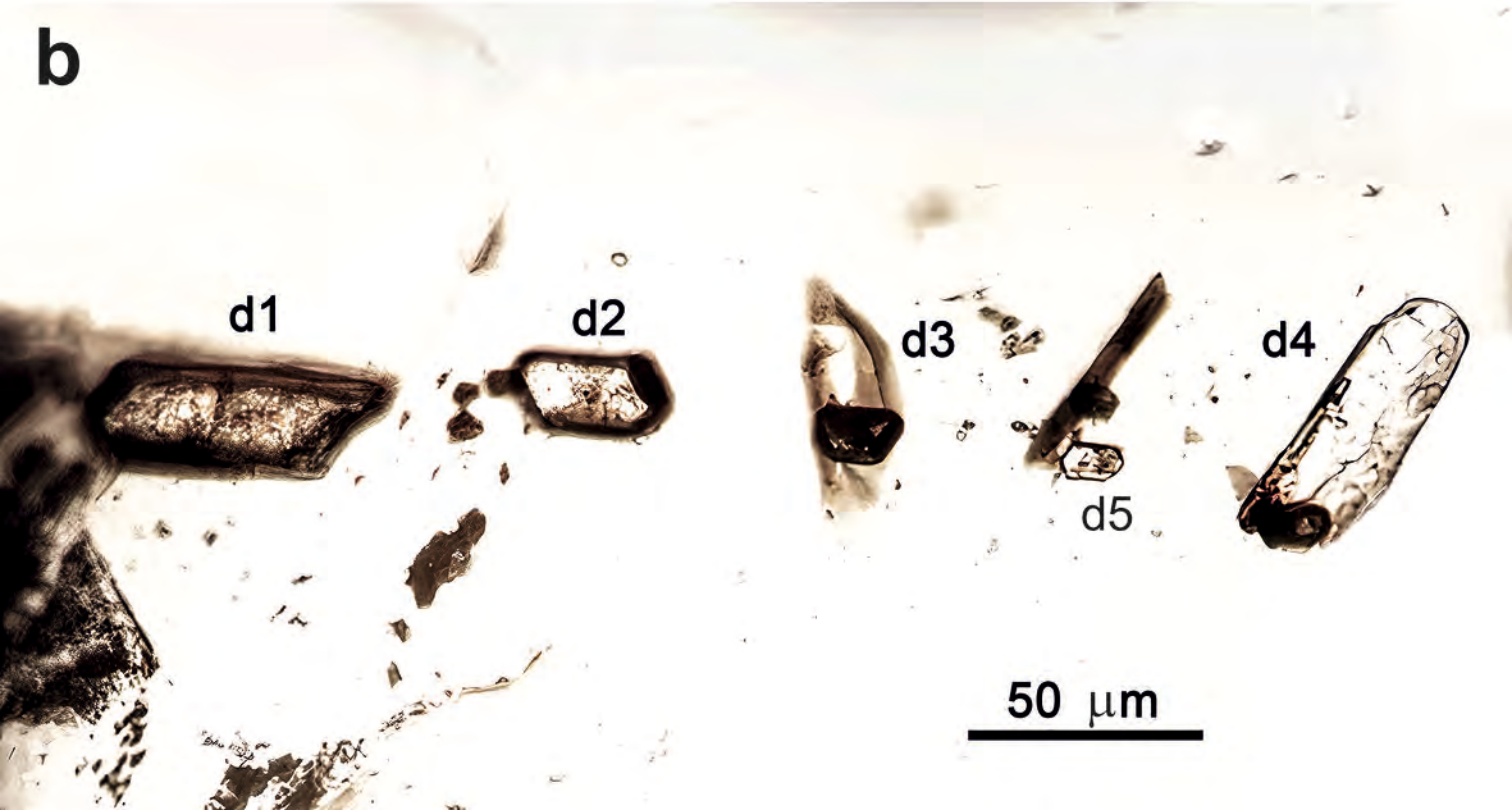

Figure 2

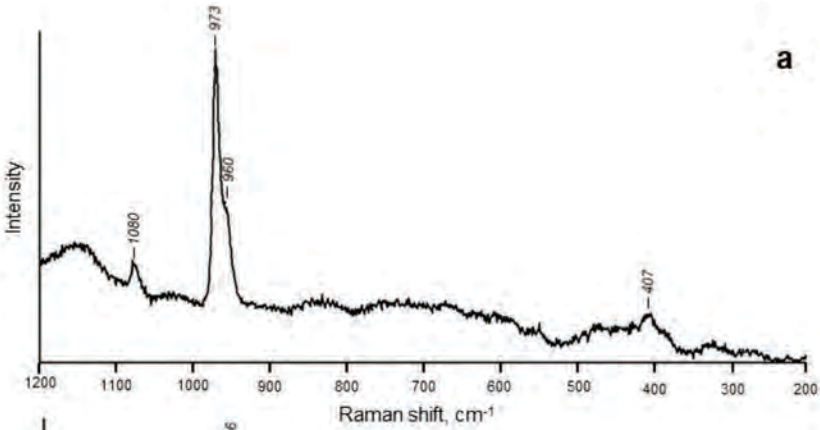
a
973
960
1080
407
Intensity
1200
1100
1000
900
800
700
600
500
400
300
200
Raman shift, cm-1

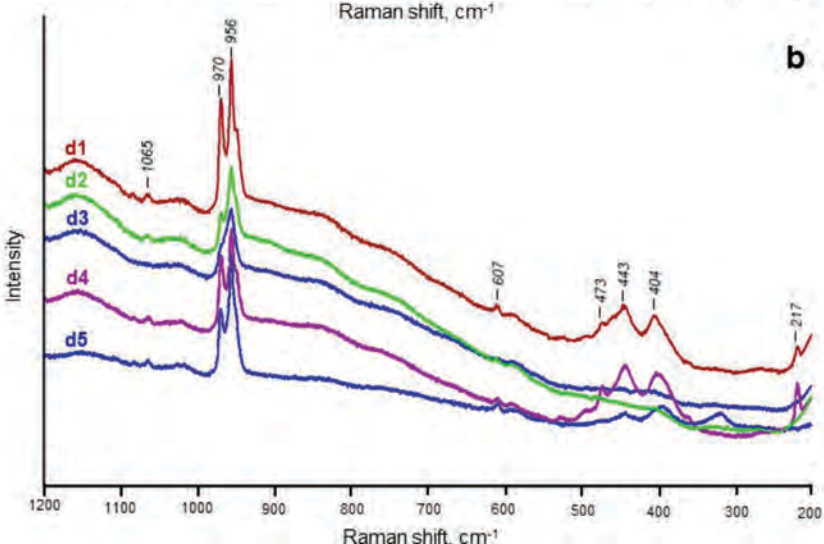
b
970
956
1065
607
473
443
404
217
d1
d2
d3
d4
d5
Intensity
1200
1100
1000
900
800
700
600
500
400
300
200
Raman shift, cm-1